THE EFFECT OF THE LOSS OF *LGL1* IN MURINE NEURAL PROGENITOR CELLS ON MAPK SIGNALING AND PROLIFERATION

By

Monique LaCourse

A Thesis Presented to

The Faculty of Humboldt State University

In Partial Fulfillment of the Requirements for the Degree

Master of Science in Biology

Committee Membership

Dr. Amy Sprowles, Committee Chair

Dr. Jenny Cappuccio, Committee Member

Dr. Jacob Varkey, Committee Member

Dr. Erik Jules, Program Graduate Coordinator

December 2018

ABSTRACT

THE EFFECT OF THE LOSS OF *LGL1* IN MURINE NEURAL PROGENITOR CELLS ON MAPK SIGNALING AND PROLIFERATION

Monique LaCourse

Glioblastoma is an incurable, aggressive, and highly invasive type of brain tumor that harbors tumor initiating cells characterized by disrupted polarized cell divisions. A cell polarity gene lethal (2) giant larvae 1 (*Lgl1*) has been implicated in gliomas and is a tumor suppressor initially identified in *Drosophila* with roles in proliferation. The loss of *Lgl1* in *Drosophila* activates the MAPK protein kinase JNK and the Ras pathway and therefore its downstream kinase ERK, a transcription factor modulator. Furthermore, when *Lgl1* is knocked out in mice, a phenotype similar to glioma is seen. Loss of the human form of *Lgl1*, *Hugl1*, and increases in c-Jun, an oncogene and JNK target, has been associated with glioma in humans. Additionally, the protooncogene transcription factor c-Myc is documented in glioma to directly correlate to tumor grade and an increase in an analogous form, d-Myc, in *Drosophila* has been shown to promote survival of *Lgl* mutants through a Ras mechanism. Here we sought to determine if the cancer properties associated with loss of *Lgl* in mice and humans are related to changes in MAPK signaling. To accomplish this, murine neural progenitor cells from the subventricular zone of mice with a *Lgl1* knockout were cultured *in vitro*. These cells were plated

adherently and characterized for changes in phosphorylation states of MAPK proteins ERK, JNK and p38 as well as two protooncogene MAPK downstream targets, c-Jun and c-Myc. In addition, to understand if MAPK phosphorylation is related to proliferation we characterized the proliferation rates of these cells in the presence of chemical inhibitors of p38 and ERK's upstream activating kinase MEK. Differential expression patterns were observed in MAPK proteins and their downstream targets associated with the loss of *Lgl1*, under standard conditions and with the treatment of DMSO as a drug vehicle control and chemical inhibitors of p38 and MEK. Additionally, it was found that the loss of *Lgl1* in neurosphere culture slightly increased growth and under adherent conditions this effect was not seen, however, changes did occur in the presence of p38 and MEK inhibitors. This supports previous data and signifies the importance of MAPK pathway in cancer phenotypes and beginning to characterize the role of the *Lgl1* protein in the mouse.

ACKNOWLEDGEMENTS

First and foremost, I would like to thank my advisor, Dr. Amy Sprowles. I would not be the person and scientist I am today without her patient guidance, knowledge, and support in completing my graduate studies. She cultivated an ideal environment for my growth as a scientist and was someone I admired and looked up to. I would also like to thank my dedicated committee members for their input: Dr. Jenny Cappuccio, Dr. Jacob Varkey, and Dr. Bruce O'Gara. Additionally, the staff of the CNRS provided essential support and supplies and I would like to thank Susan Wright, Marty Reed, Liz Weaver, Lewis McCrigler, Brandon Wilcox, Michelle Dostal, Darrel Burlison, Stephanie Steffen, and Dave Baston.

Dr. Claudia Petritsch's lab at UCSF collaborated on this project and provided the cells. Previous research on this project was crucial for its inception and was completed by Hannah Collins, Abigail Petersen, and Jacqueline Trzeciak. Additionally, I worked along side fellow graduate student, Sharon Otis, in optimizing and designing the experiments performed. Without their work this project would not be possible.

TABLE OF CONTENTS

LIST OF TABLES

LIST OF FIGURES

LIST OF APPENDICES

INTRODUCTION

Glioblastoma Origins in Neural Stem and Progenitor Like Cells

Glioblastomas comprise approximately 17% of central nervous system tumors which are incurable, aggressive, and highly invasive. Their diffuse nature makes surgery impossible and chemotherapy and radiation treatments rarely increase the mean patient survival of 14 months (Phuphanick 2017). A characteristic feature which makes them difficult to treat is their phenotypic heterogeneity due to the glioblastoma cells existing in different differentiation states (Singh et al. 2004). Genetically-engineered mouse models have shown glioblastoma tumors to harbor stem-cell like tumor propagating cells originating from neural stem and progenitor cells which upon transplantation to an immunocompromised mouse have the ability to regenerate the tumor (as reviewed by Liebelt et al. 2016; Singh et al. 2004; Llaguno et al. 2009; Sugiarto et al. 2011). These undifferentiated cells are resistant to current radiation and chemotherapy treatments signifying they have a key role in glioblastoma recurrence and show the need for further research to develop treatments to target these cells (Bao et al. 2006; Chen et al. 2012). Additionally, human and murine glioblastoma tumor propagating cells are characterized by disrupted polarized cell divisions, increased self-renewal, and impaired differentiation capacities (Sugiarto et al. 2011). Better understanding the molecular mechanisms behind these cancer properties could provide insight into the etiology and treatments for this devastating cancer.

Lethal Giant Larvae Homolog 1 as a Highly Conserved Cell Polarity Gene

Loss of cell polarity is considered a hallmark of cancer formation and cell proliferation. Mutations in genes governing asymmetric cell division and apical-basal cell polarity promote tumor formation in *Drosophila* and mammals (reviewed in Neumuller and Knoblich 2009). One of these genes is lethal (2) giant larvae homolog 1 (*Lgl1*), which is a membrane bound tumor suppressing protein with roles in cell polarity and proliferation that is conserved across the eukaryotic kingdom (Gateff 1978; Mechler et al. 1985; Lee et al. 2006; Humbert et al. 2003). The gene was initially characterized in *Drosophila* through a genetic screen which found it to contribute to larval morphology deformities by being a recessive regulator of malignant neuroblastomas. It was named for its extraordinary ability to create fatal overgrowth in the brain and imaginal discs in *Drosophila* (Gateff 1978). It was later identified in *Drosophila* this dysregulation in symmetrical division occurred in neuroblasts, stem cells of the developing brain, due to a signaling disruption between *Lgl*, Pins, and aPKC (Lee et al. 2006). There are two mammalian homologues, *Lgl1* (*Hugl1*) and *Lgl*2 (*Hugl2*). Similarities in their roles is related to the conserved structure in the *Lgl* protein across different species consisting of multiple WD40 domains which are used as a scaffold for coordination of multiprotein complex assemblies and contain serine and threonine phosphorylation sites.

Lgl in *Drosophila* Development

Mutations in *Drosophila* lethal giant larvae gene (D-*Lgl*) causes loss of apical-basal polarity, loss of epithelial organization, and uncontrolled proliferation (Baek 1999; Bilder 2001; Humbert et al. 2003; Justice et al. 2003). D-*Lgl* co-localizes with Discs-large (Dlg) and Scribble to establish and maintain the basolateral domain while functioning competitively with protein complexes that are necessary for the apical membrane domain, the Par complex (Par3/Par6/aPKC) and Crumbs complex (Crumbs/Pals/Patj) (Bilder and Perrimon 2000; Ohshiro et al. 2000; Peng et al. 2000; Albertson and Doe 2003; Betschinger et al. 2003; Tanentzapf and Tepass 2003). D-*Lgl* acts together with Numb, a negative regulator of Notch, a protein related to glial differentiation and self-renewal of the neural progenitor cell (Betschinger et al. 2003). Depletion of *Lgl* upregulates Notch signaling in *Drosophila* eye tissue and increased Notch has been noted to prevent differentiation and encourages undifferentiated proliferation (Parsons et al. 2014). In the Hippo pathway, which has roles in proper control of cell survival and organ size, loss of *Lgl* causes deregulation potentially inducing tumorous tissue growth through an increase in Yorkie activity (Grzeschik et al. 2010; Froldi et al. 2010). Similarly, an increase in Yorkie activity is also seen through upregulation of one of the mitogen activated protein kinases (MAPK), Jun N-terminal kinase (JNK) (Sun and Irvine 2013). This work in *Drosophila* has led to many mammalian studies to characterize the differences between species and further elucidate *Lgl*'s role in development and pathology.

Lgl1 in Mammalian Development and Pathology

Studies shifted to mammalian model after the promising studies in *Drosophila* in hopes to uncover a treatment for pathologies related to *Lgl*. *Lgl1* is broadly expressed in mice with the highest expression in the brain (Klezovitch et al. 2004). Numb mutant mice display hyperplasia of the developing cortex (Li et al. 2003). Also related to increased Notch signaling, in transgenic mice the *Lgl1* gene product controls cell cycle exit and apical-basal polarity of neural progenitor cells. This results in aberrant growth and symmetric cell division of neuroepithelial cells forming a phenotype similar to glioma partly due to their inability to differentiate (Klezovitch et al. 2004) (Figure 1). In humans, it has been suggested that normal polarity signaling is necessary for maintenance of healthy tissue and disrupted cell polarity may contribute to epithelial-to-mesenchymal transition and tumorigenesis (Shin et al. 2006; Nakaya and Sheng 2013; Casarsa et al. 2011). However, *Lgl*'s role in leukemia has been inconsistent and the absence of *Lgl1* in mice does not alter leukemiai by Notch, c-Myc, and Jak2 signaling (Hawkins et al. 2014). Recent data has suggested opportunities for further research on the mechanism may lie in the mitochondria related signaling, MAPK and Ras signaling, and mTor signaling (reviewed in Cao et al. 2015). Overall there remains a gap in truly understanding the mechanism of action of *Lgl1* and its role in cancer particularly in mammalian models such as mice which showed such a severe and fatal phenotype with the loss of *Lgl1* (Klezovitch et al. 2004).

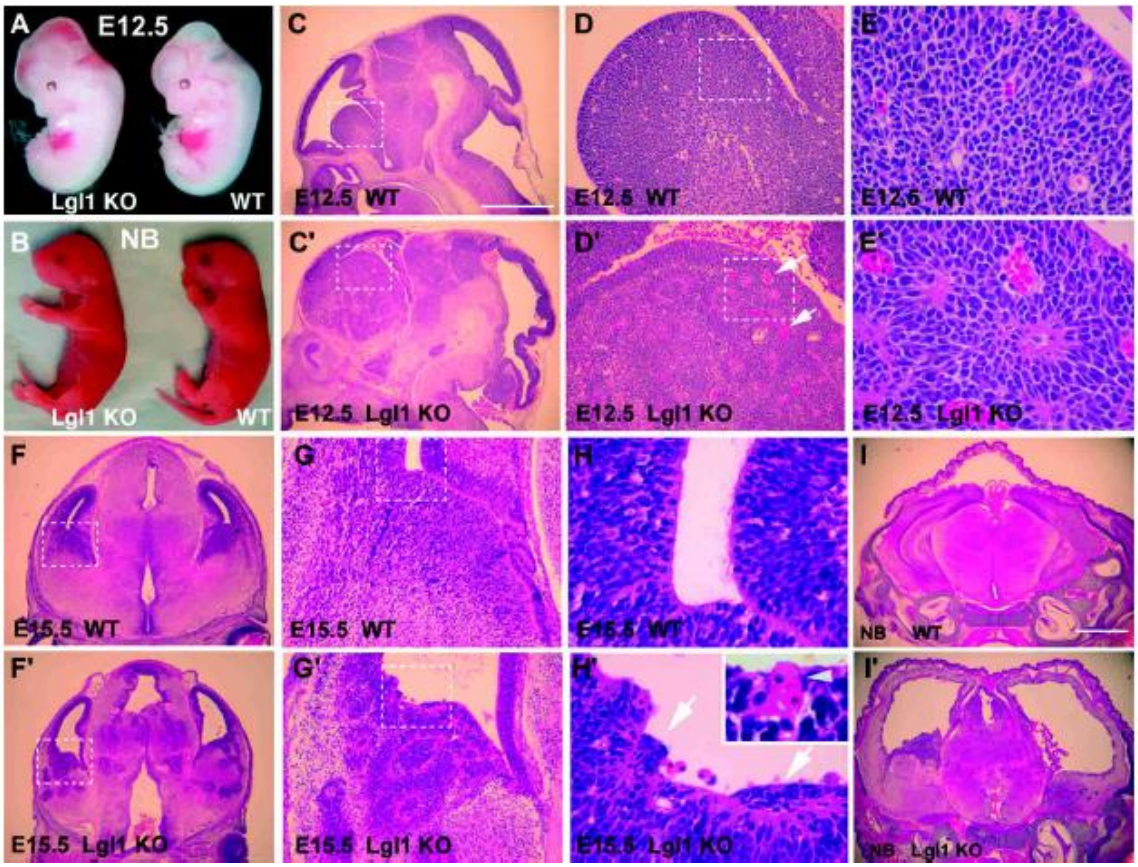

Figure 1. *In vivo* murine *Lgl1* knockout displays overgrowth of the brain**.** (A, B) Changes to the morphology of E12.5 mouse embryos with Lgl1 loss. (C, C' through E, E') Histological changes in brain structure compared to WT samples of E12.5 embryos. D, D' and E, E' represent magnified images of the previous boxed areas. (F, F' through H, H') Histological changes in brain structure compared to WT samples of E15.5 embryos. G, G' and H, H' represent magnified images of the previous boxed areas. Inset of H' shows an aberrantly localized blood vessel on the ventricular wall. (I, I') Visualization of ventricle dilation and damage with loss of *Lgl1* function (adapted from Klezovitch et al. 2004).

Hugl-1 in Human Glioma

The molecular mechanisms of the human homolog of *Lgl* is still being understood in various tissue types and cancers. It has been found that *Hugl1* suppresses various epithelial cancers by inhibiting proliferation and migration and promoting apoptosis and cell adhesions (Lu et al. 2009; Song et al. 2013; Kuphal et al. 2006). One study found decreased levels of *Hugl1* in human glioma tissues, indicating it is involved in glioma progression. However, over-expression *in vitro* either stably or transiently did not affect glioma cell proliferation or regulate the Hippo pathway as suggested in the *Drosophila* model. In an orthotopic model of nude mice with a glioma cell line, over-expression of *Hugl1* inhibited gliomagenesis and proliferation and promoted apoptosis (Liu et al. 2015). Furthermore, *Hugl1* is constitutively phosphorylated and inactivated in glioblastoma cells. Cell motility and invasion of glioblastoma cells was reduced *in vitro* and *in vivo*, respectively, and differentiation promoted *in vitro* and *in vivo* when a non-phosphorylatable and constitutively active form of *Lgl1* was expressed in a glioblastoma cell line, in primary patient cells, and in intracerebral xenografts (Gont et al. 2014). Phosphorylation of *Hugl1* was attributed to increased aPKC activity from increased PI 3-kinase due to the loss of PTEN of which this loss occurs in 90% of glioblastomas (Gont 2016). While this data supports previous work in *Drosophila,* the molecular mechanism of action is still not fully understood in humans and certainly not in mice.

Mitogen Activated Protein Kinase (MAPK) Pathway

Mitogen-activated protein kinases (MAPKs) are serine-threonine kinases that mediate intracellular signaling associated with a variety of cellular activities including cell proliferation, differentiation, survival, death, and transformation (McCubrey et al. 2006; Dhillon et al. 2007). The mammalian MAPK family consists of p38, extracellular signal-regulated kinase (ERK), and c-Jun N-terminal kinase (JNK). They are comprised of several isoforms: ERK1 to ERK8; p38-α, -β, -γ, and -δ; and JNK1, 2 and 3 (Schaeffer and Weber 1999). Each signaling axis to activate these MAPK proteins consists of three components which phosphorylate each other in the following order: a MAPK kinase kinase (MAP3K) phosphorylates a MAPK kinase (MAP2K) which in turn phosphorylates the MAPK. Activated MAPKs phosphorylate various substrate proteins including transcription factors such as Elk-1, c-Jun, ATF2, and p53 (reviewed in Kim and Choi 2010).

MAPKs have been implicated in numerous functions in many types of cancer with cancerous mutations being primarily associated with the Ras/Raf/MEK/ERK pathway while the stress activated pathways, JNK and p38, appear to counteract malignant formation (reviewed in Dhillon et al. 2007). A summary of the MAPK pathway can be found in Figure 2. Roles for each have been documented in the properties associated with glioblastoma.

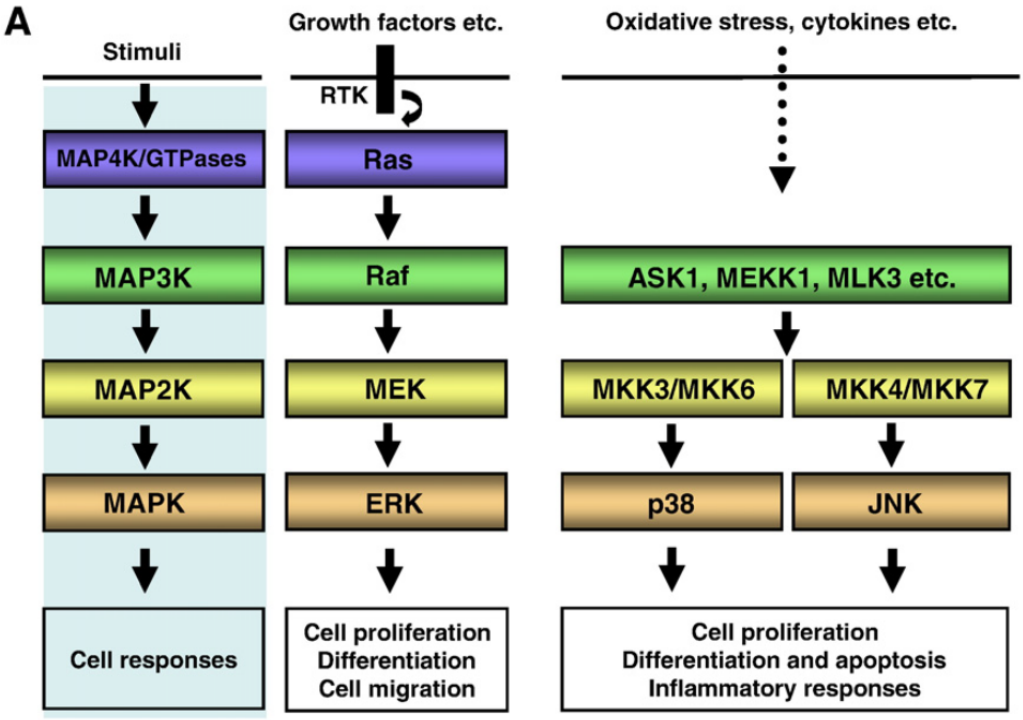

Figure 2. Mitogen-activated protein kinase (MAPK) signaling pathways. MAPK signaling pathways mediate intracellular signaling initiated by extracellular or intracellular stimuli. MAP3Ks, which are activated by MAP4Ks or GTPases, mediate phosphorylation and activation of MAP2Ks, which in turn phosphorylate and activate MAPKs. Activated MAPKs phosphorylate various substrate proteins including transcription factors, resulting in regulation of a variety of cellular activities including cell proliferation, differentiation, migration, inflammatory responses, and death. The mammalian MAPK family includes ERK, p38, and JNK (adapted from Kim and Choi 2010).

MAPK in relation to *Lgl1*, neural stem cells, and glioblastoma

ERK. The RAF/ERK signaling pathway is activated during neural stem cell proliferation and neuronal and astrocytic differentiation (Rhee et al. 2016). Additionally, the phosphorylation of ERK is necessary for neuronal differentiation and survival of differentiating cells (Li et al. 2007). The RAS/RAF/MEK/ERK signaling cascade is implicated in a number of cancers and therefore a common target for chemotherapies and is even referred to as the "Achilles heel of the MAPK pathway in cancer therapy" (Liu et al. 2018). Mutations in upstream kinase MEK has led to hyper activation of ERK and been shown to induce gliomas *in vivo* with the additional activation of AKT or loss of Ink4a/Arf. Recently a large genomic screening of various grades of diffuse glioma tissue found a substantial amount of activating KRAS and NRAS mutations (Ceccarelli et al. 2016). Furthermore, glioma cell proliferation is controlled by ERK activity-dependent surface expression of PDGFRA in glioma cells. Treatment with a MEK inhibitor induced an initial inhibition of ERK1/2 phosphorylation, followed by up-regulated ERK1/2 phosphorylation concomitant with diminished surface expression of PDGFRA which decreased cell proliferation (Chen et al. 2014). Curcumin was found to effect glioma cell line by activating the ERK pathway and inducing autophagy. When the ERK pathway was inhibited the curcumin-induced autophagy was inhibited thus enhancing cytotoxicity (Aoki et al. 2007). PKC isoforms differentially effect ERK with PKC α inducing the activation of nuclear ERK and PKC ε inducing the activation of ERK at focal adhesions to mediate glioma cell adhesion and motility (Besson et al. 2001).

p38. MAPK p38 has been found to have varying roles in different tissues in relation to inflammation, development, and cancer progression (Bradham and McClay 2006). A p38 scaffold protein assembly induces the of expression of gene programs for neurogenesis and endogenous p38 has been found to promote migration of adult neural stem/progenitor cells (Oh et al. 2009; Hamanoue et al. 2016). Additionally, p38 phosphorylate Dlg to promotes it localization to the membrane where it combines with *Lgl* to maintain cell polarity (Sabio et al. 2005). The invasive and progressive nature of glioma has been linked to MKK3 and subsequently p38 activation. The inhibition of either of these significantly reduced invasiveness *in vitro* and greatly sensitized glioma cells to cytotoxic therapies (Demuth et al. 2007). Finally, p38 and JNK pathways were shown to affect VEGF secretion in malignant glioma cells; therefore, possibly contributing to VEGF-induced angiogenesis (Yoshino et al. 2006).

JNK. Jun N-terminal kinase (JNK) has a known role in cancer; however, JNK1 and 2 have shown to have different and sometimes opposing roles in different tissues (Bubici and Papa 2014). JNK1 was found to have an important role in neural development as knockout mice had aberrant phenotypes (Kuan et al. 1999). In *Drosophila*, the loss of *Lgl* is associated with increased phosphorylation of JNK that results apoptosis (Di Giacomo et al. 2017; Froldi et al. 2010; Menendez et al. 2010; Grifoni et al. 2015). Furthermore, phosphorylation of JNKs and c-Jun has been shown to strongly correlate with the histological grade of glioblastoma and poor prognosis (Li et al. 2008). Elevated levels of JNKs activity was observed in glioblastoma cell lines and in human tumor tissues with JNK2 having the most pro-tumorigenic role in glioblastoma in

comparison to JNK1 and 3 (Antonyak et al. 2002; Li et al. 2008). Sphere and monolayer culture conditions were evaluated for human glioma stem cell lines. It was found that JNK signaling and sphere culture was crucial for the maintenance of stemness. JNK2 was again found to be the most important isoform to maintain stemness and increased phosphorylation of it and subsequently increased Notch signaling was found in spheres in comparison with monolayer culture conditions (Yoon et al. 2012). Additionally, JNK activity is required for the maintenance of stem-like glioblastoma cells. In this study, human glioma cells were xenografted into mice and a transient and systemic JNK inhibitor administered. As a result, there was a depletion of self-renewing and tumor-initiating populations, inhibition of tumor formation by stem-like glioblastoma cells in the brain, and it provided a survival benefit with minimal adverse effect (Matsuda et al. 2012).

c-Jun and Myc. c-Jun and Myc are both proto-oncogenes transcription factors downstream of MAPKs. c-Jun is activated by JNK through phosphorylation at Ser63, Ser73, Thr91, and Thr93; and by ERK and p38 via increased gene expression (Chang and Karin 2001). While Myc activation has been tied to the MAPK family (Zhu et al. 2008). In *Drosophila,* poor survival of *Lgl* mutants due to p-JNK mediated apoptosis was rescued when dMyc expression or RAS activity was high (Froldi et al. 2010; Menendez et al. 2010; Grifoni et al. 2015). Therefore, Myc-mediated cell competition was proposed for cancer survival where there is a direct relationship between fitness and Myc expression in relation to Hugl (Di Giacomo et al. 2017). Along with this levels of Myc correlated directly with tumor grade and therefore prognosis (Herms et al. 1999). Myc

inhibition *in vivo* and and *in vitro* for both murine and human cell lines and tissues reduced proliferation and increased apoptosis (Annibali et al. 2014). On the other hand, it was found that c-Jun accumulation in glioblastoma was not due to MAPK signaling but IRES mediated cap-independent translation (Blau et al. 2012).

In Summary

There is evidence that the MAPK family and oncogenes, c-Jun and c-Myc, are involved with *Lgl* and glioma to promote cancer survival, progression, and apoptosis. However, the molecular mechanisms connecting the dots between various pathways are poorly understood and therefore targeted drugs with minimal adverse effects are difficult to develop. Additionally, it remains unclear whether loss of polarity is a consequence of uncontrolled proliferation or a causative factor in cancer initiation. To further elucidate the effects of these proteins and proliferation in relation to *Lgl*, we will use murine neural progenitor cells with *Lgl1* knocked out and MAPK small molecule inhibitors. Specifically, SB203580 will be used to inhibit the phosphorylation of p38 by binding to the ATP-binding pocket and PD0325901 to inhibit MEK and therefore its downstream targets such as ERK1/2.

STATEMENT OF AIMS

These aims are designed to elucidate the role of *Lgl1* in the mouse in relation to MAPK signaling and proliferation. There is a strong correlation with cell polarity in cancer phenotypes and *Lgl1*'s role in the brain. It is not known the molecular mechanisms behind *Lgl1*'s role in glioma like phenotypes in the mouse and how proliferation relates. A summary of the experimental design to accomplish these aims can be found in Figure 3.

1.) Does loss of *Lgl1* affect MAPK signaling?

This aim is designed to evaluate the effect of the loss of *Lgl1* in murine neural progenitor cells on MAPK signaling pathways. We hypothesized there would be changes to MAPK signaling specifically an increase in activity with the loss of *Lgl1*. To evaluate this, murine neural progenitor cells isolated from the subventricular zone of neonatal mice with the *Lgl1* gene knocked out were cultured under conditions that support the analysis of growth and proliferation. Total cytoplasmic protein was isolated from these cells cultured either under standard conditions or in the presence of MAPK inhibitors. Immunoblots for the endogenous and phosphorylated forms of MAPKs were evaluated. Fold changes were calculated from the normalized densitometry values to evaluate the effect of the loss of *Lgl1* and MAPK inhibitors.

2.) Does loss of *Lgl1* affect expression and phosphorylation of classic MAPK targets involved in proliferation and cancer?

This aim is designed to characterize MAPK activity by evaluating the effect of the loss of *Lgl1* in murine neural progenitor cells on classic MAPK targets through immunoblot analysis. We hypothesized there would be increased expression and phosphorylation of oncogenes c-Jun and c-Myc correlated with an increase in MAPK activity.As described in Aim 1, total nuclear proteins were isolated from these cells after treatment with MAPK inhibitors followed by a fold change analysis of the normalized densitometry values.

3.) Does loss of *Lgl1* change proliferation alone and/or in the presence of MAPK inhibitors in primary murine neural progenitor cells?

This aim is designed to evaluate the effect of loss of *Lgl1* alone and/or in the presence of MAPK inhibitor in murine neural progenitor cells on proliferation as an adherent culture. We hypothesized the loss of *Lgl1* would increase proliferation and this increase would not be seen when the MAPKs are inhibited. The cells were plated adherently in a 96 well plate in quadruplicate alone and in the presence of MAPK inhibitors. The CyQuant cell proliferation assay was used to assess cell growth over 96 hours with a fluorometric output based on DNA content.

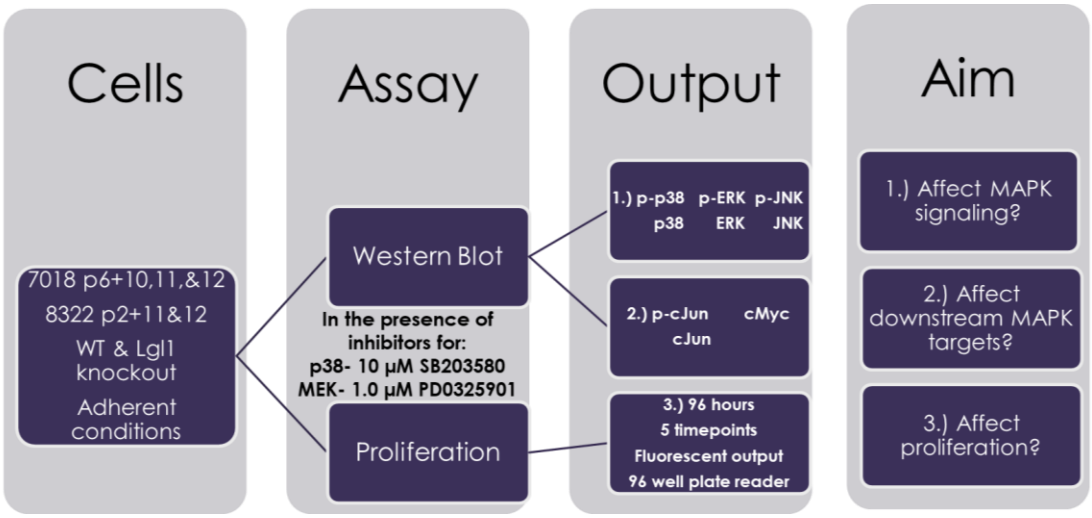

Figure 3. Experimental design. Neural progenitor cells from the subventricular zone of mice 7018 and 8322 with *Lgl1* knocked out were plated adherently and treated with an inhibitor for p38, 10 µM SB203580, and an inhibitor for MEK, 1.0 µM PD0325901. Immunoblots were used to evaluate the first and second aim designed to see if the loss of *Lgl1* changes MAPK signaling or their downstream targets, c-Jun and c-Myc. To evaluate the third aim of the effect of *Lgl1* on proliferation a 96-well fluorescent proliferation assay was used.

METHODS

Neural Progenitor Cell Maintenance Culture Conditions

Primary neural progenitor cells were isolated from the subventricular zone of adult *Lgl1*$^{loxp/loxp}$ mice (Klezovitch et al. 2004) by a postdoctoral fellow in the Petritsch laboratory at UCSF's Helen Diller Cancer Center. The cells were treated with adenovirus containing either GFP or GFP-Cre to create genetically matched *Lgl1*$^{+/+}$ and *Lgl1*$^{-/-}$ primary neural progenitor cells for biological replicates 7018 and 8322 at passage six and two, respectively. The cells were propagated and maintained as neurospheres in ultra-low adherent vessels at a density of 25,000 cells/mL in neurobasal-A medium (Gibco #10888022) supplemented with 1:50 vitamin B27 without vitamin A (Gibco #12587010) and 1:100 L-glutamine (Gibco #25030081) along with epidermal growth factor (Sigma Aldrich #E9644) and fibroblast growth factor (Pepro-Tech #100-18B) every other day. They were incubated at 37°C and passaged when the spheres started to darken in the center every 4-6 days with Accutase (Corning #MT25058Cl) at 37°C for 5-8 minutes. They were cryopreserved in basal media supplemented with 10% DMSO and 20% BIT 9500.

Adherent Culture Conditions

Biological replicate 7018 at passage 10, 11, and 12 and 8322 at passage 11 and 12 were used for adherent conditions. Replicates 7018 p10 and the passage 11 cells came from cryopreservation then cultured as spheres for 5 days prior to being harvested for

adherent culture. The passage 11 cells were then plated back and continued as spheres for harvest and plating as adherent at passage 12. Culture vessels were coated with poly-L-ornithine (Millipore A-004-C) at 15 µg/mL in phosphate buffered saline (PBS) for 30 minutes at room temperature, washed three times with PBS, then coated with laminin (Corning #354239) at 6.1 µg/mL in PBS at 37°C for 3 hours. Cells were maintained as spheres for 5 days except for 8322 p2+12 for 6 days. A single cell solution was prepared with Accutase by straining the cells with a 37-micrometer strainer (STEMCELL #27250). Biological replicate 7018 at passage 10, 11, and 12 and 8322 at passage 11 and 12 were plated adherently at 30,000 cells/cm^2 for 24 hours prior to treatment. Cells cultured under standard conditions were evaluated for the effects of *Lgl1* only. To assess how loss of *Lgl1* affected p38 and ERK signaling, cells were cultured in SB203580 at 10 µM (Adipogen Syn-1074) or PD0325901 at 1.0 µM (SelleckChem S1036). The inhibitors were dissolved in DMSO (Tocris 31-762) and applied to the cells at 1:2000; therefore, a drug vehicle control culture received DMSO at 1:2000.

Immunoblots

Cells were harvested with Accutase (Corning #MT25058Cl) after 2 hours of treatment with inhibitors and pelleted for protein extraction. NE-PER Nuclear and Cytoplasmic Extraction Reagents were used to extract cytoplasmic and nuclear protein, then the proteins were quantified with a BCA assay according to manufacturer instructions (Thermo Fisher #78835, #23227). Proteins were denatured at 95°C for 5 minutes in 6x Laemmli buffer. Samples were run at 110 volts at 4°C in precast Novex 10-

20% Tris-glycine gels (Invitrogen #XP10205) in 1X SDS running buffer. Proteins were transferred to a PVDF membrane activated in 100% methanol (Millipore #IPVH00010) in cold transfer buffer (1X Tris-Gly Buffer, 20% Methanol and ddH2O to volume) at 20V for 2-8 hours at 4°C. The membrane was place in blocking buffer (1X TBST, 1% BSA and 0.1% nonfat milk) for 15 minutes on a rocker prior to primary antibody diluted in blocking buffer being applied and incubated overnight at 4°C. Primary antibodies applied were c-Jun, p-c-Jun (Ser63), c-Myc, p38, p-p38, ERK, p-ERK, JNK, p-JNK, and GAPDH (Appendix A). After washing the membrane three times in 1X TBST on a rocker, a horseradish (HRP) peroxidase conjugated secondary protein (Thermo Fisher #31460) was applied for 1 hour diluted 1:2000 in blocking buffer at room temperature. Following three more washes in 1X TBST the blot was developed with WesternSure Premium Chemiluminescent Substrate (Li-Cor #C50528-02) prepared at a 1:1 ratio immediately prior to imaging with the Li-Cor-C-Digital blot scanner. GAPDH was used as a loading control and initial blots were run with 1.5-2 µg protein to confirm concentration by densitometry. Nuclear blots were loaded with 3-5 µg of protein and cytoplasmic with 8-10 µg protein. Following the imaging of the primary antibody, all blots were acid stripped (Thermo Fisher #21059) for 5-10 minutes to obtain a GAPDH loading control for each gel run. After stripping the membrane was washed for thoroughly three times on a rocker, blocked again for 15 minutes, and GAPDH primary antibody applied at 1:2000 for 1 hour at room temperature. Secondary antibody application and imaging steps remain the same. Densitometry was performed with Image Studio and Microsoft Excel used to analyze the output.

Proliferation Assay

Plates with 96-wells were coated for adherent culture and a single cell suspension prepared and plated as detailed above with a multi-channel pipettor. Cells were allowed to adhere for 4 hours before the first time point was taken and DMSO or drugs were added as detailed above. Each time point was run in quadruplicate and due to the nature of the reagents, a separate set of cells were plated for each timepoint. The CyQuant NF Cell Proliferation Assay Kit was utilized, and plates were visualized with a Spectramax i3 Plate Reader.

Data Analysis

Western blot

Densitometry values were obtained with Image Studio. Values of proteins of interest were normalized to conserved glycolysis gene, GAPDH, and phosphorylated forms of the proteins were also normalized to their endogenous protein level. Fold changes were calculated between genotype, $Lgl1^{-/-}/Lgl1^{+/+}$, for no treatment. To evaluate the treatments and control for the effect of drug vehicle, first the fold change between treatment within genotype was calculated as follows: DMSO/NT, SB/DMSO, and PD/DMSO. Those fold change values were used to create a fold change between genotype, $Lgl1^{-/-}/Lgl1^{+/+}$. Heat maps were created according to the color values recorded in Table 1. Additionally, a one sample t-test was performed on the log of the fold change values with a p-value of 0.05.

Proliferation

The most dissimilar value from the average was removed from all quadruplicates before the fluorescent output values were averaged. Fold changes for the different conditions and heat maps were created in the same manner as the western blots. Additionally, a one sample t-test was performed on the log of the fold change values with a p-value of 0.05.

Table 1. Fold change heat map key. Key for fold change heat maps of western blot densitometry values and proliferation fluorescence output. The miniscule effect was only evaluated in the proliferation data.

Heat Map Key		
Fold Change Range	**Color**	**Indication**
≥ 2.0		Increase
= 1.8- 2.0		Mild increase
= 1.5- 1.8		Slight increase
= 1.3- 1.5		Miniscule increase
= 0.85- 1.3		No effect
= 0.75- 0.85		Miniscule decrease
= 0.6- 0.75		Slight decrease
= 0.5- 0.6		Mild decrease
≤ 0.5		Decrease
N/A		Not present or evaluated
≤ 0.25 or ≥ 4.0	*	Strong decrease or increase

RESULTS

Sphere Culture Propagation and Harvest

Neural progenitor cells were maintained and propagated as spheres for 5 days except 8322 p12 for 6 days due to slow and abnormal growth. Cells were harvested with 92.5- 98.9% viability as determined by trypan blue prior to plating under adherent conditions after 5 days of growth (Appendix D). The loss of *Lgl1* slightly increased sphere growth except in 7018 p11 with an average fold change of 1.34 including 7018 p11 and 1.44 excluding 7018 p11 (Appendix E).

Loss of *Lgl1* Affects MAPK Signaling

Low yields of protein extract were obtained particularly in cells treated with PD0325901 (MEK/ERK inhibitor), of higher passage, and in 8322. Cells of passage 12 and in particular 8322 had less cells adhered after 24 hours in comparison to 7018 and passage 10 and 11. Furthermore, upon addition of PD0325901 for 2 hours, the majority of cells were no longer adhered. Therefore, data for c-Jun, JNK1/2/3, and p-JNK1/2/3 is not complete for all replicates. In particular, c-Jun was not evaluated in 7018 p11 for any treatment and in 8322 for cell treated with PD0325901 in $Lgl1^{-/-}$. Additionally, JNK was not evaluated in 8322 and p-JNK was not evaluated in 8322 p12.

Immunoblot data was highly variable across replicates. Despite fold changes of at least 1.5 or 0.75 in multiple replicates, a one sample t-test on the log of the fold changes revealed few genes with a significant change due to the loss of *Lgl1* (p-value ≤ 0.05).

With a p-value of 0.05, the loss of *Lgl1* significantly affected the phosphorylation of p38 when normalized to p38 (t= 2.80, df= 4, p-value= 0.049) in the presence of a p38 inhibitor, 10 µM SB203580, and the phosphorylation of JNK p54 when normalized to GAPDH (t= 10.34, df= 2, p-value= 0.009) in the presence of a MEK inhibitor, 1.0 µM PD0325901 (Table 2). Additionally, 7018 p10 lacked a p-JNK p54 band and a band slightly larger than p-p38 was visualized in 7018 p11 for cells treated with SB203580 only and in all treatments for 8322 p11 (Appendix H, J).

Overall, the loss of *Lgl1* and inhibitors affecting the MAPK pathway did not have an effect on endogenous levels of MAPK proteins. The loss of *Lgl1* had no effect on p38 and JNK levels and a preferential decrease in 8322 of ERK1/2. In the presence of DMSO, there was no effect on p38 except a slight decrease in passage 11, an increase in ERK1, a preferential increase in 8322 of ERK2, no effect in 7018 in JNK p54, and a slight decrease in JNK1/2/3 p54 in 7018. In the presence of a p38 or MEK inhibitor there was no effect on p38, ERK1/2, and JNK p46/p54 (7018 only) (Figure 4).

Table 2. Minimal significant changes to MAPK signaling with the loss of *Lgl1*. The p-values from a one sample two-tailed t-test on log fold change of densitometry values of western blots from adherent cultures treated for 2 hours with nothing, 1:2000 DMSO, 10 µM SB203580 (p38 inhibitor), and 1.0 µM PD0325901 (MEK inhibitor). Densitometry values of proteins of interest were normalized to GAPDH and the phosphorylated forms also normalized to their endogenous levels. Fold changes were calculated between genotype, $Lgl1^{-/-}/Lgl1^{+/+}$, for no treatment. To evaluate the treatments and control for the effect of drug vehicle, first the fold change between treatment within genotype was calculated as follows: DMSO/NT, SB/DMSO, and PD/DMSO. Those fold change values were used to create a fold change between genotype, $Lgl1^{-/-}/Lgl1^{+/+}$. Bolded text indicates a significant change due to loss of *Lgl1* with a p-value of 0.05 or less.

		1- sample t-test p-value			
Norm to:	Gene	NT	DMSO 1:2000	SB203580 10 µM	PD0325901 1.0 µM
GAPDH	cJun	0.369	0.339	0.400	0.172
GAPDH	p-cJun	0.137	0.087	0.544	0.524
cJun	p-cJun	0.280	0.057	0.617	0.387
GAPDH	c-Myc	0.382	0.138	0.284	0.589
GAPDH	p38	0.893	0.454	0.238	0.678
GAPDH	p-p38	0.442	0.588	0.464	0.361
p38	p-p38	0.442	0.655	**0.049**	0.482
GAPDH	ERK1	0.048	0.520	0.140	0.491
GAPDH	p-ERK1	0.894	0.872	0.426	0.452
ERK	p-ERK1	0.588	0.851	0.087	0.151
GAPDH	ERK2	0.158	0.135	0.257	0.660
GAPDH	p-ERK2	0.434	0.977	0.612	0.588
ERK	p-ERK2	0.276	0.319	0.750	0.521
GAPDH	JNK p54	0.979	0.525	0.352	0.542
GAPDH	p-JNK p54	0.196	0.771	0.181	**0.009**
JNK	p-JNK p54	0.225	0.911	0.438	0.141
GAPDH	JNK p46	0.586	0.743	0.268	0.366
GAPDH	p-JNK p46	0.067	0.437	0.847	0.941
JNK	p-JNK p46	0.224	0.774	0.825	0.846

A.)

Proliferation Fold Change			
NT	7018		8322
	p11	p12	p11
24/24	1.00	1.00	1.00
48/24	1.29	0.92	1.24
72/24	1.04	1.59	0.99
96/24	1.34	1.91	0.70

Western Fold Change						
NT		7018			8322	
Norm to:	Gene	p10	p11	p12	p11	p12
GAPDH	cJun	0.772		0.815	1.21	0.856
GAPDH	p-cJun	0.56	0.449	0.546	1.566	0.604
cJun	p-cJun	0.726		0.67	1.294	0.705
GAPDH	c-Myc	0.799	0.883	0.886	1.382	0.599
GAPDH	p38	0.808	1.27	0.836	1.473	0.865
GAPDH	p-p38	1.082	1.449	0.533	0.683	0.835
p38	p-p38	1.34	1.141	0.637	0.463	0.965
GAPDH	ERK1	0.7	0.803	1.017	0.519	0.724
GAPDH	p-ERK1	3.035	0.086	1.62	1.35	2.788
ERK	p-ERK1	4.335	0.107	1.593	2.599	3.85
GAPDH	ERK2	0.99	0.798	1.102	0.483	0.664
GAPDH	p-ERK2	3.287	0.172	2.391	1.91	5.034
ERK	p-ERK2	3.32	0.216	2.169	3.951	7.58
GAPDH	JNK p54	1.472	0.788	0.877		
GAPDH	p-JNK p54		1.044	0.999	2.017	
JNK	p-JNK p54		1.326	1.139		
GAPDH	JNK p46	1.078	0.764	0.994		
GAPDH	p-JNK p46	1.951	2.125	0.968	0.830	
JNK	p-JNK p46	1.811	2.783	0.974		

B.)

Proliferation Fold Change			
DMSO /NT	7018		8322
	p11	p12	p11
24/24	1.00	1.00	1.00
48/24	0.74	1.16	0.67
72/24	0.88	1.10	0.84
96/24	0.75	0.97	1.05

Western Fold Change						
DMSO/NT		7018			8322	
Norm to:	Gene	p10	p11	p12	p11	p12
GAPDH	cJun	1.128		0.224	0.879	0.856
GAPDH	p-cJun	1.085	0.528	0.144	0.48	0.604
cJun	p-cJun	0.962		0.642	0.547	0.705
GAPDH	c-Myc	0.714	0.109	0.109	0.454	1.734
GAPDH	p38	0.872	0.745	1.448	0.662	0.922
GAPDH	p-p38	0.862	0.946	5.806	0.717	0.918
p38	p-p38	0.988	1.271	4.008	0.463	0.996
GAPDH	ERK1	1.698	0.848	0.915	2.148	0.74
GAPDH	p-ERK1	0.37	1.924	2.103	0.942	0.93
ERK	p-ERK1	0.218	2.269	2.299	0.438	1.256
GAPDH	ERK2	0.929	0.915	1.866	2.784	1.672
GAPDH	p-ERK2	0.542	2.103	1.43	0.806	0.789
ERK	p-ERK2	0.584	2.299	0.767	0.289	0.472
GAPDH	JNK p54	0.349	1.273	0.924		
GAPDH	p-JNK p54		0.813	1.295	0.232	
JNK	p-JNK p54		0.639	1.401		
GAPDH	JNK p46	0.738	1.437	0.733		
GAPDH	p-JNK p46	0.314	0.552	2.291	0.732	
JNK	p-JNK p46	0.426	0.384	3.127		

C.)

Proliferation Fold Change			
SB/ DMSO	7018		8322
	p11	p12	p11
24/24	1.00	1.00	1.00
48/24	0.70	0.77	2.71
72/24	0.96	0.81	2.33
96/24	0.91	0.84	1.44

Western Fold Change						
SB/DMSO		7018			8322	
Norm to:	Gene	p10	p11	p12	p11	p12
GAPDH	cJun	2.461		3.606	0.73	0.761
GAPDH	p-cJun	0.801	2.306	6.14	0.394	1.065
cJun	p-cJun	0.325		1.703	0.539	1.399
GAPDH	c-Myc	1.764	1.952	7.246	0.654	0.828
GAPDH	p38	1.064	0.934	1.176	1.119	2.341
GAPDH	p-p38	0.707	1.142	0.33	0.724	1.707
p38	p-p38	0.665	0.153	0.28	0.648	0.729
GAPDH	ERK1	0.876	1.146	0.328	0.529	0.776
GAPDH	p-ERK1	1.525	0.781	0.674	1.632	1.963
ERK	p-ERK1	1.742	0.682	2.058	3.086	2.53
GAPDH	ERK2	1.096	1.09	0.421	0.787	0.799
GAPDH	p-ERK2	0.59	0.702	0.495	1.743	1.413
ERK	p-ERK2	0.538	0.644	1.177	2.214	1.768
GAPDH	JNK p54	0.497	0.855	1.05		
GAPDH	p-JNK p54		0.77	0.357	2.205	
JNK	p-JNK p54		0.901	0.34		
GAPDH	JNK p46	0.939	0.852	1.005		
GAPDH	p-JNK p46	2.139	1.138	0.469	1.334	
JNK	p-JNK p46	2.277	1.335	0.467		

D.)

Proliferation Fold Change			
PD/ DMSO	7018		8322
	p11	p12	p11
24/24	1.00	1.00	1.00
48/24	0.52	1.10	0.97
72/24	1.05	0.81	0.65
96/24	1.00	0.56	0.41

Western Fold Change						
PD/DMSO		7018			8322	
Norm to:	Gene	p10	p11	p12	p11	p12
GAPDH	cJun	0.127		0.412		
GAPDH	p-cJun	0.726	2.905	3.288	0	0.771
cJun	p-cJun	3.636		1.045		
GAPDH	c-Myc	1.358	1.694	7.043	0	0.661
GAPDH	p38	1.162	0.902	1.56	0.975	0.362
GAPDH	p-p38	0.55	1.233	0.394	2.096	0.238
p38	p-p38	0.473	1.367	0.253	2.149	0.657
GAPDH	ERK1	0.654	1.146	0.931	1.468	2.024
GAPDH	p-ERK1	0.568	0.781	1.006	1.341	0.925
ERK	p-ERK1	0.869	0.682	1.08	0.913	0.457
GAPDH	ERK2	0.846	1.362	0.924	1.091	1.043
GAPDH	p-ERK2	1.499	1	0.595	1.048	1.924
ERK	p-ERK2	1.771	1	0.643	0.961	1.845
GAPDH	JNK p54	0.301	1.26	1		
GAPDH	p-JNK p54		0.809	0.756		
JNK	p-JNK p54		0.643	0.756		
GAPDH	JNK p46	1.045	0.994	1.433		
GAPDH	p-JNK p46	2.043	1.016	0.518		
JNK	p-JNK p46	1.955	1.022	0.362		

Figure 4. The loss of *Lgl1* affects MAPK signaling and downstream targets, c-Jun and c-Myc. Heat maps (refer to Table 1 for key) of fold changes between genotype ($Lgl1^{-/-}$/$Lgl1^{+/+}$) for western blot densitometry values and proliferation fluorescent output data for adherent cultures from mice 7018 and 8322 at passage 10, 11, and 12. Westerns were normalized to GAPDH and the phosphorylated form to the endogenous protein of interest. Proliferation data was collected over 96 hours with data points every 24 hours; this data was normalized to the 24-hour time point. Treatments/inhibitors were added at plating for proliferation and after 24 hours for westerns; they were then normalized to the drug vehicle control, DMSO, to control for its affect. A.) Represents data for no treatment (NT) where the culture was adhered for 26 hours. B.) Represents data for DMSO, the drug vehicle, at 1:2000 after 2 hours in culture normalized to NT to evaluate its affect. C.) Represents data for cells treated with 10 µM SB203580 for 2 hours and normalized to the drug vehicle, DMSO at 1:2000. D) Represents data for cells treated with 1.0 µM PD0325901 for 2 hours and normalized to the drug vehicle, DMSO at 1:2000.

The loss of *Lgl1* had no effect on phosphorylation of p38, an increase in phosphorylation of ERK1/2, a preferential increase in 8322 of phosphorylation of p-JNK p54 in, and an increase in the phosphorylation of JNK p46. In the presence of DMSO, the loss of *Lgl1* had no effect on the phosphorylation of p38 and JNK p54 and a decrease in phosphorylation of ERK1/2 and JNK p46. DMSO reverses the effect of the loss of *Lg1l* in no treatment with ERK1/2 and JNK p46 from increased to decreased levels. The p38 and MEK inhibitors had increased sensitivity with the loss of *Lgl1* decreased the phosphorylation of p38 and ERK in comparison to no treatment. In the presence of a p38 inhibitor, the loss of *Lgl1* decreased phosphorylation of p38, increased phosphorylation on ERK1, increased phosphorylation of ERK2 in 7018 and decreased it 8322, and was inconclusive on the phosphorylation of JNK. In the presence of a MEK inhibitor (effect of drug vehicle controlled), the loss of *Lgl1* decreased the phosphorylation of p38, had no effect on the phosphorylation of ERK1 and JNK p54, and was inconclusive for the phosphorylation of ERK2 and JNK 46 (Figure 4).

Loss of *Lgl1* Affects the Expression and Phosphorylation of c-Jun and c-Myc

For reasons mentioned above, due to lack of sample, c-Jun was not evaluated in 7018 p11 for any treatment and in 8322 for cells treated with PD0325901 in $Lgl1^{-/-}$. Additionally, the loss of *Lgl1* in the presence of the MEK inhibitor, 1.0 μM PD0325901, in 8322 p11 completely shuts down the phosphorylation of c-Jun at serine 63 and c-Myc levels (Figure 5).

Overall, the MEK inhibitor drastically decreased the amount of c-Jun in *Lgl1*$^{-/-}$cells. As well as c-Myc levels and the phosphorylation of c-Jun at serine 63 in both genotypes and preferentially in the *Lgl1*$^{-/-}$cells and in 8322. The p38 inhibitor, 10 μM SB203580, also decreased c-Jun and c-Myc levels and affected the phosphorylation of c-Jun. DMSO had a notable effect on the *Lgl1*$^{-/-}$cells by decreasing c-Myc levels and the phosphorylation of c-Jun. While the loss of *Lgl1* alone had no effect on c-Jun and c-Myc levels and a decrease on the phosphorylation of c-Jun. In the presence of DMSO, there was no effect on c-Jun levels and a decrease in c-Myc and the phosphorylation of c-Jun. The p38 inhibitor increases c-Jun and c-Myc levels preferentially in 7018 and decreases phosphorylation of c-Jun. The MEK inhibitor decreases c-Jun levels, affects the phosphorylation of c-Jun, and increases c-Myc levels in 7018 while decreasing them in 8322 (Figure 4).

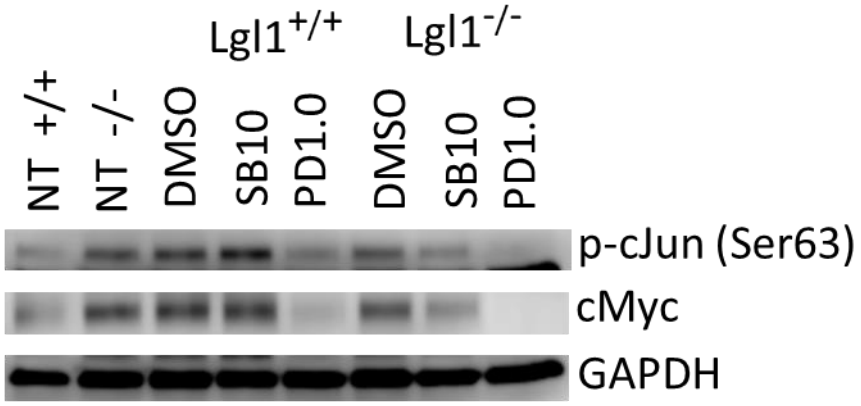

Figure 5. MEK inhibitor, PD0325901 at 1.0 μM, completely inhibits phosphorylation of c-Jun and expression of c-Myc in 8322 p11 in *Lgl1*$^{-/-}$cells. Immunoblot normalized to GAPDH from biological replicate 8322 p11 under adherent conditions following 2 hours of treatment with inhibitors. Labels are defined as follows: no treatment (NT), DMSO at 1:2000 (DMSO), 10 μM SB203580 (SB10), 1.0 μM PD0325901 (PD1.0).

Exceptions of note exist in data generated from replicate 7018 p11 which had an anomalous strong decrease in the phosphorylation of ERK1/2 with the loss of *Lgl1* and in the presence of DMSO an increase in the phosphorylation of ERK1/2. Additionally, in 7018 p12 in the presence of DMSO, a decrease in c-Jun and c-Myc levels were associated with an increase in ERK1 levels and the phosphorylation of p38 and JNK1. The opposite effect was seen in 7018 p12 in the presence of a p38 inhibitor where there is an increase in c-Jun and c-Myc levels (Figure 4).

Loss of *Lgl1* Affects Proliferation

The proliferation assay was performed under neurosphere and adherent culture conditions. Spheres tended to clump together more in 96 well plates and the reagent for the assay could not fully penetrate the spheres leading to inconsistent data. Therefore, adherent culture conditions were used to evaluate proliferation and MAPK signaling with western blots. No significant difference in proliferation was seen with the loss of *Lgl1* under any treatment with a p-value of 0.05 (Table 3).

Table 3. No significant change in proliferation with the loss of *Lgl1*. One sample two-tailed t-test p-values for fold change ($Lgl1^{-/-}/Lgl1^{+/+}$) of proliferation rates of spheres over 5 days of growth and adherent culture over 4 days of growth normalized to the 24-hour timepoint. In sphere data, 8322 p12 was excluded since it grew for 6 days. In proliferation data, 7018 p10 and 8322 p12 were excluded due to loss of potency in reagents. Adherent cultures were allowed to adhere for 4 hours prior to treatment with nothing (NT), DMSO (1:2000), 10 µM SB203580 (SB), and 1.0 µM PD0325901 (PD). Fold changes were calculated between genotype, $Lgl1^{-/-}/Lgl1^{+/+}$, for no treatment and sphere data. To evaluate the treatments and control for the effect of drug vehicle, first the fold change between treatment within genotype was calculated as follows: DMSO/NT, SB/DMSO, and PD/DMSO. Those fold change values were used to create a fold change between genotype, $Lgl1^{-/-}/Lgl1^{+/+}$. With a p-value of 0.05 there was no significant change in proliferation due to the loss of *Lgl1*.

Proliferation 1- sample t-test p-values		
Culture condition	**Treatment**	**P-value**
Sphere	NT	0.057
Adherent	NT	0.572
	DMSO	0.477
	SB	0.872
	PD	0.202

Adherent proliferation data on 7018 p10 and 8322 p12 was discarded due to the light and temperature sensitive reagents losing potency. The loss of *Lgl1* caused a slight increase in proliferation in sphere culture which was not found in adherent culture except in 7018 p12 (Figure 6). In the presence of DMSO, there was a slight decrease in proliferation with the loss of *Lgl1* in adherent culture except in 7018 p12. The addition of a p38 inhibitor only caused an increase in 8322 p11 and in the presence of a MEK inhibitor decreased proliferation in all replicates and preferentially in 8322 (Figure 4, 7).

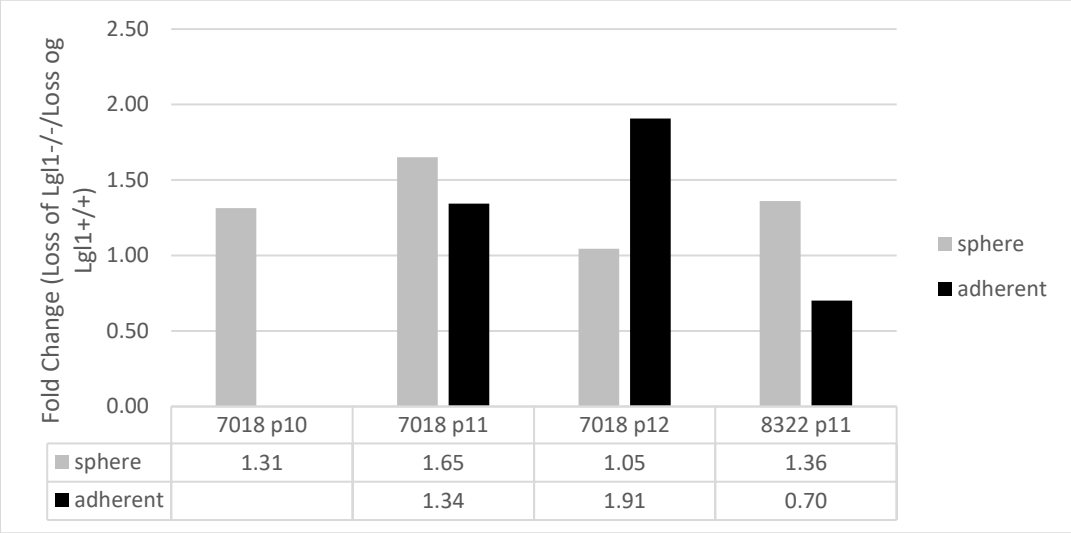

Figure 6. The loss of *Lgl1* causes a slight increase in proliferation in sphere culture conditions. Fold change ($Lgl1^{-/-}/Lgl1^{+/+}$) of proliferation rates of spheres over 5 days of growth and adherent culture over 4 days of growth normalized to the 24-hour timepoint. The loss of *Lgl1* slightly increases the proliferation of spheres in comparison to adherent culture conditions except in 7018 p12.

Proliferation Fold Change												
	7018 p11				7018 p12				8322 p11			
	24/24	48/24	72/24	96/24	24/24	48/24	72/24	96/24	24/24	48/24	72/24	96/24
NT	1.00	1.29	1.04	1.34	1.00	0.92	1.59	1.91	1.00	1.24	0.99	0.70
DMSO/NT	1.00	0.74	0.88	0.75	1.00	1.16	1.10	0.97	1.00	0.67	0.84	1.05
SB/DMSO	1.00	0.70	0.96	0.91	1.00	0.77	0.81	0.84	1.00	2.71	2.33	1.44
PD/DMSO	1.00	0.52	1.05	1.00	1.00	1.10	0.81	0.56	1.00	0.97	0.65	0.41

Figure 7. Inconsistent changes in proliferation with the loss of *Lgl1* under adherent culture conditions. Heat map of fold change ($Lgl1^{-/-}/Lgl1^{+/+}$) of proliferation data. Spheres were grown for 5 days and adherent cultures for 4 days and normalized to the 24 hour timepoint. Cultures were allowed to adhere for 4 hours prior to treatment with nothing, DMSO (1:2000), SB203580 (10 µM), and PD0325901 (1.0 µM). Fold changes were calculated between genotype, $Lgl1^{-/-}/Lgl1^{+/+}$, for no treatment and sphere data. To evaluate the treatments and control for the effect of drug vehicle, first the fold change between treatment within genotype was calculated as follows: DMSO/NT, SB/DMSO, and PD/DMSO. Those fold change values were used to create a fold change between genotype, $Lgl1^{-/-}/Lgl1^{+/+}$. The color in the replicate label reflects the fold change of the sphere growth.

The increase in proliferation seen with a p38 inhibitor in 8322 p11 was associated with an anomalous decrease in c-Jun and c-Myc levels and the phosphorylation of c-Jun. The decrease in proliferation seen in the presence of an MEK inhibitor was associated with a decrease in c-Jun levels. The preferential decrease in proliferation in 8322 p11 with the MEK inhibitor was associated with a decrease in c-Myc levels that was preferential in 8322 and an anomalous increase in phosphorylation of p38 (Figure 7).

DISCUSSION

We found differential expression patterns associated with the loss of *Lgl1* in MAPK proteins and their downstream targets under standard conditions and with the treatment of DMSO and chemical inhibitors of p38 (10 μM SB203580) and MEK/ERK (1.0 μM PD0325901). Additionally, changes to growth and proliferation were found due to the loss of *Lgl1* in the presence of p38 and ERK inhibitors. These results signify the importance of MAPK pathway in cancer phenotypes and the beginning of characterizing the role of *Lgl1* in the mouse.

Loss of *Lgl1* Affects MAPK Signaling

Immunoblot analysis shows loss of *Lgl1* increased the amount of phosphorylated ERK in both 7018 and 8322 cell lines and a preferential increase in p-JNK p54 in 8322 (Figure 4A). The drug vehicle, DMSO, had a significant effect on ERK levels and the phosphorylation levels of ERK and JNK. DMSO has been found to have a significant effect on development of embryonic stem cells with morphological changes to embryoid bodies and downregulation of stemness factors (Pal et al. 2011). Additionally, hyperosmotic stress induced by the addition of DMSO in HeLA cells was found to result in the breakage of the cortical cytoskeleton and the detachment of the cell membrane from the cortical cytoskeleton, causing the formation of cell blebs (Ruan et al. 2015). In melanoma cells, continued exposure to DMSO resulted in cytoskeletal reorganization characterized by thick and regularly oriented microfilament bundles that led to increased

adhesion to the substrate and inhibited cell growth (Lampugnani et al. 1987). In this experiment, passage 12 had an extra passage of sphere propagation from cryopreservation where they were exposed to DMSO as well, another source of variation between replicates.

The cells were plated on poly-L-ornithine which has been shown to promote differentiation through an ERK mediated mechanism. p-ERK has also been found to be necessary for differentiation (Ge et al. 2015). Additionally, 8322 had lower protein yields which could suggest a p-JNK- induced apoptosis often seen with the loss of *Lgl1* in *Drosophila* if there is not an increase in c-Myc (Di Giacomo et al. 2017). DMSO reversed the effects seen under standard conditions with ERK and JNK and decreased c-Myc, a stemness marker. This could be explained by the effect DMSO has on differentiation and its associated decrease of stemness markers (Pal et al. 2011).

The inhibitors were functional and preferential with the loss of *Lgl* indicating that MAPKs affect cellular functions differently with the loss of *Lgl*. Unfortunately, due to the biological variation between replicates and not deep enough of an analysis, the molecular mechanism was not able to be determined. Of note there was an increase in phosphorylation of ERK2 in 7018 and decreased it 8322 which could be associated to the more sensitive nature of 8322 due to the knockout being induced at an earlier passage. In the presence of a MEK inhibitor the loss of *Lgl1* decreased the phosphorylation of p38 potentially indicating a loss in the invasive ability of the cells.

We did not observe consistent upregulation of JNK or an increase the phosphorylation of JNK which has been noted numerous times (Yoon et al. 2012; Di Giacomo et al. 2017; Grifoni et al. 2015; Froldi et al. 2010; Menendez et al. 2010). This could be attributed to the monolayer conditions as reported in Yoon et al. 2012. Biological replicate 8322 and in particular passage 12 grew oddly as spheres and upon harvest had low protein yields. Unfortunately, the low protein yields led to insufficient protein to evaluate JNK in order to test the hypothesis that p-JNK is related to apoptosis.

Variation seen in the replicates could be attributed to differences in the mice and isolates from their brains since the cells were not sorted. Additionally, 8322 had the knockout induced at p2 and 7018 at p6. In both sphere and adherent culture 8322's were consistently more sensitive and less robust. Furthermore, these cells were primary cells approaching higher passages. They have been culture by many different students over the years with varying reagents before being used for these experiments. In this study, it was attempted to minimize this variation by harvesting the samples over 3 weeks with one person performing the experiments and culturing them with reagents from the same lot number.

Loss of *Lgl1* Affects c-Jun and c-Myc

Blau et al. 2012 found that changes in c-Jun were not consistently associated with changes in MAPK signaling in glioblastoma which would support an alternative translation model. They found that c-Jun protein accumulation was not associated with an increase in c-Jun mRNA. Instead a potent internal ribosome entry site was discovered

that direct cap-independent translation in glioblastoma cells (Blau et al. 2012). The changes observed could be associated with alternative translation.

The strongest increase in c-Myc due to the loss of *Lgl1* occurred in the presence of the p38 inhibitor in 7018 p12. This correlated with the strongest decrease in p-JNK p46 and an increase p-ERK which would support previous data which c-Myc promotes survival in relation to an increase in RAS activity and the cells are rescued from p-JNK initiated apoptosis (Grifoni et al. 2015).

The loss of *Lgl1* Affects Proliferation

The loss of *Lgl1* in spheres slightly increased proliferation indicating a stemness property that was seen in a previous study that compared sphere and monolayer culture in glioblastoma cell lines (Yoon et al. 2012). The MEK inhibitor decreased proliferation in both genotypes and preferentially with the loss of *Lgl1*, indicating a potential treatment for *Lgl1* related cancers.

SUMMARY

Further experimentation must be completed to conclusively determine MAPK's role in relation to *Lgl1* with statistical relevance. It would useful to be able to differentiate between the JNK isoforms and focus on the role of JNK2 (Yoon et al. 2012). Sphere culture should be revisited due to the effects of adherent substrates and data supporting stemness in spheres. Glioma stem cells could be obtained and *Lgl1* knocked down and overexpressed while performing the same experimental design. *In vivo* studies in the mouse evaluating these pathways would be of interest to remove the artifacts of *in vitro* studies. Immunohistochemistry on *Lgl1* knockout mouse brains for MAPKs and their targets could reveal a clearer role or possible stratification in the overgrowth. Coupled with immunohistochemistry of post-mortem human glioblastoma tumors for comparison of signaling and patterns within the tumor.

Many Ras/Ref/MEK/ERK inhibitors are being developed and explored for use in treating a number of different cancers. However, just as the MEK inhibitor, PD0325901 at 1.0 μM, had extreme effects on the cells used in this experiment, a lot of inhibitors comes with similar devastating side effects *in vivo*. Understanding in greater detail how mutations and activations in that pathway function will help to create a more targeted drug.

REFERENCES

- Albertson R, Doe CQ. 2003. Dlg, Scrib and Lgl regulate neuroblast cell size and mitotic spindle asymmetry. Nature cell biology. 5(2):166.
- Annibali D, Whitfield JR, Favuzzi E, Jauset T, Serrano E, Cuartas I, Redondo-Campos S, Folch G, Gonzàlez-Juncà A, Sodir NM, Massó-Vallés D. 2014. Myc inhibition is effective against glioma and reveals a role for Myc in proficient mitosis. Nature communications. 5:4632.
- Antonyak MA, Kenyon LC, Godwin AK, James DC, Emlet DR, Okamoto I, Tnani M, Holgado-Madruga M, Moscatello DK, Wong AJ. 2002. Elevated JNK activation contributes to the pathogenesis of human brain tumors. Oncogene. 21(33):5038.
- Aoki H, Takada Y, Kondo S, Sawaya R, Aggarwal B, Kondo Y. 2007. Evidence that curcumin suppresses the growth of malignant gliomas in vitro and in vivo through induction of autophagy: role of Akt and ERK signaling pathways. Molecular pharmacology. 72(1):29-39.
- Baek KH. 1999. The first oncogene in Drosophila melanogaster. Mutation Research/Reviews in Mutation Research. 436(2):131-6.
- Bao S, Wu Q, McLendon RE, Hao Y, Shi Q, Hjelmeland AB, Dewhirst MW, Bigner DD, Rich JN. 2006. Glioma stem cells promote radioresistance by preferential activation of the DNA damage response. Nature. 444(7120):756.
- Besson A, Davy A, Robbins SM, Yong VW. 2001. Differential activation of ERKs to focal adhesions by PKC ε is required for PMA-induced adhesion and migration of human glioma cells. Oncogene. 20(50):7398.
- Betschinger J, Mechtler K, Knoblich JA. 2003. The Par complex directs asymmetric cell division by phosphorylating the cytoskeletal protein Lgl. Nature. 422(6929):326.
- Bilder D. 2001. Cell polarity: squaring the circle. Current Biology. 11(4):R132-5.
- Bilder D, Li M, Perrimon N. 2000. Cooperative regulation of cell polarity and growth by Drosophila tumor suppressors. Science. 289(5476):113-6.
- Blau L, Knirsh R, Ben-Dror I, Oren S, Kuphal S, Hau P, Proescholdt M, Bosserhoff AK, Vardimon L. 2012. Aberrant expression of c-Jun in glioblastoma by internal ribosome entry site (IRES)-mediated translational activation. Proceedings of the National Academy of Sciences. 109(42):E2875-84.
- Bradham C, McClay DR. 2006. p38 MAPK in development and cancer. Cell cycle. 5(8):824-8.
- Bubici C, Papa S. 2014. JNK signalling in cancer: in need of new, smarter therapeutic targets. British journal of pharmacology. 171(1):24-37.

- Cao F, Miao Y, Xu K, Liu P. 2015. Lethal (2) giant larvae: an indispensable regulator of cell polarity and cancer development. International Journal of Biological Sciences. 11(4):380.
- Casarsa C, Bassani N, Ambrogi F, Zabucchi G, Boracchi P, Biganzoli E, Coradini D. 2011. Epithelial-to-mesenchymal transition, cell polarity and stemness-associated features in malignant pleural mesothelioma. Cancer letters. 302(2):136-43.
- Ceccarelli M, Barthel FP, Malta TM, Sabedot TS, Salama SR, Murray BA, Morozova O, Newton Y, Radenbaugh A, Pagnotta SM, Anjum S. 2016. Molecular profiling reveals biologically discrete subsets and pathways of progression in diffuse glioma. Cell. 164(3):550-63.
- Chang L, Karin M. 2001. Mammalian MAP kinase signalling cascades. Nature. 410(6824):37.
- Chen J, Li Y, Yu TS, McKay RM, Burns DK, Kernie SG, Parada LF. 2012. A restricted cell population propagates glioblastoma growth after chemotherapy. Nature. 488(7412):522.
- Chen D, Zuo D, Luan C, Liu M, Na M, Ran L, Sun Y, Persson A, Englund E, Salford LG, Renström E. 2014. Glioma cell proliferation controlled by ERK activity-dependent surface expression of PDGFRA. PLoS One. 9(1):e87281.
- Demuth T, Reavie LB, Rennert JL, Nakada M, Nakada S, Hoelzinger DB, Beaudry CE, Henrichs AN, Anderson EM, Berens ME. 2007. MAP-ing glioma invasion: mitogen-activated protein kinase kinase 3 and p38 drive glioma invasion and progression and predict patient survival. Molecular cancer therapeutics. 6(4):1212-22.
- Dhillon AS, Hagan S, Rath O, Kolch W. 2007. MAP kinase signalling pathways in cancer. Oncogene. 26(22):3279.
- Di Giacomo S, Sollazzo M, Paglia S, Grifoni D. 2017. MYC, cell competition, and cell death in cancer: The inseparable triad. Genes. 8(4):120.
- Froldi F, Ziosi M, Garoia F, Pession A, Grzeschik NA, Bellosta P, Strand D, Richardson HE, Pession A, Grifoni D. 2010. The lethal giant larvae tumour suppressor mutation requires dMyc oncoprotein to promote clonal malignancy. BMC biology. 8(1):33.
- Gateff E. 1978. Malignant neoplasms of genetic origin in Drosophila melanogaster. Science. 200(4349):1448-59.
- Ge H, Tan L, Wu P, Yin Y, Liu X, Meng H, Cui G, Wu N, Lin J, Hu R, Feng H. 2015. Poly-L-ornithine promotes preferred differentiation of neural stem/progenitor cells via ERK signalling pathway. Scientific reports. 5:15535.
- Gont A. 2016. *Inactivation of Lgl1 in Glioblastoma* (Doctoral dissertation, Université d'Ottawa/University of Ottawa).
- Gont A, Hanson JE, Lavictoire SJ, Daneshmand M, Nicholas G, Woulfe J, Kassam A, Da Silva VF, Lorimer IA. 2014. Inhibition of glioblastoma malignancy by Lgl1. Oncotarget. 5(22):11541.

- Grzeschik NA, Parsons LM, Allott ML, Harvey KF, Richardson HE. 2010. Lgl, aPKC, and Crumbs regulate the Salvador/Warts/Hippo pathway through two distinct mechanisms. Current biology. 20(7):573-81.
- Grifoni D, Bellosta P. Drosophila Myc: a master regulator of cellular performance. 2015. Biochimica et Biophysica Acta (BBA)-Gene Regulatory Mechanisms. 1849(5):570-81.
- Hamanoue M, Morioka K, Ohsawa I, Ohsawa K, Kobayashi M, Tsuburaya K, Akasaka Y, Mikami T, Ogata T, Takamatsu K. 2016. Cell-permeable p38 MAP kinase promotes migration of adult neural stem/progenitor cells. Scientific reports. 6:24279.
- Hawkins ED, Oliaro J, Ramsbottom KM, Ting SB, Sacirbegovic F, Harvey M, Kinwell T, Ghysdael J, Johnstone RW, Humbert PO, Russell SM. 2014. Lethal giant larvae 1 tumour suppressor activity is not conserved in models of mammalian T and B cell leukaemia. PloS one. 9(1):e87376.
- Herms JW, von Loewenich FD, Behnke J, Markakis E, Kretzschmar HA. 1999. c-Myc oncogene family expression in glioblastoma and survival. Surgical neurology. 51(5):536-42.
- Humbert P, Russell S, Richardson H. 2003. Dlg, Scribble and Lgl in cell polarity, cell proliferation and cancer. Bioessays. 25(6):542-53.
- Justice N, Roegiers F, Jan LY, Jan YN. 2003. Lethal giant larvae acts together with numb in notch inhibition and cell fate specification in the Drosophila adult sensory organ precursor lineage. Current biology. 13(9):778-83.
- Kim EK, Choi EJ. 2010. Pathological roles of MAPK signaling pathways in human diseases. Biochimica et Biophysica Acta (BBA)-Molecular Basis of Disease. 1802(4):396-405.
- Klezovitch O, Fernandez TE, Tapscott SJ, Vasioukhin V. 2004. Loss of cell polarity causes severe brain dysplasia in Lgl1 knockout mice. Genes & development. 18(5):559-71.
- Kuan CY, Yang DD, Roy DR, Davis RJ, Rakic P, Flavell RA. 1999. The Jnk1 and Jnk2 protein kinases are required for regional specific apoptosis during early brain development. Neuron. 22(4):667-76.
- Kuphal S, Wallner S, Schimanski CC, Bataille F, Hofer P, Strand S, Strand D, Bosserhoff AK. 2006. Expression of Hugl-1 is strongly reduced in malignant melanoma. Oncogene. 25(1):103.
- Lampugnani MG, Pedenovi M, Niewiarowski A, Casali B, Donati MB, Corbascio GC, Marchisio PC. 1987. Effects of dimethyl sulfoxide (DMSO) on microfilament organization, cellular adhesion, and growth of cultured mouse B16 melanoma cells. Experimental cell research. 172(2):385-96.
- Lee CY, Robinson KJ, Doe CQ. 2006. Lgl, Pins and aPKC regulate neuroblast self-renewal versus differentiation. Nature. 439(7076):594.
- Li A, Walling J, Kotliarov Y, Center A, Steed ME, Ahn SJ, Rosenblum M, Mikkelsen T, Zenklusen JC, Fine HA. 2008. Genomic changes and gene

expression profiles reveal that established glioma cell lines are poorly representative of primary human gliomas. Molecular Cancer Research. 6(1):21-30.

- Li HS, Wang D, Shen Q, Schonemann MD, Gorski JA, Jones KR, Temple S, Jan LY, Jan YN. 2003. Inactivation of Numb and Numblike in embryonic dorsal forebrain impairs neurogenesis and disrupts cortical morphogenesis. Neuron. 40(6):1105-18.
- Li J, Wang G, Wang C, Zhao Y, Zhang H, Tan Z, Song Z, Ding M, Deng H. 2007. MEK/ERK signaling contributes to the maintenance of human embryonic stem cell self-renewal. Differentiation. 75(4):299-307.
- Liebelt BD, Shingu T, Zhou X, Ren J, Shin SA, Hu J. 2016. Glioma stem cells: signaling, microenvironment, and therapy. Stem cells international. 2016:7849890.
- Liu X, Lu D, Ma P, Liu H, Cao Y, Sang B, Zhu X, Shi Q, Hu J, Yu R, Zhou X. 2015. Hugl-1 inhibits glioma cell growth in intracranial model. Journal of neuro-oncology. 125(1):113-21.
- Liu F, Yang X, Geng M, Huang M. 2018. Targeting ERK, an Achilles' Heel of the MAPK pathway, in cancer therapy. Acta pharmaceutica sinica B. 8(4):552-562.
- Llaguno SA, Chen J, Kwon CH, Jackson EL, Li Y, Burns DK, Alvarez-Buylla A, Parada LF. 2009. Malignant astrocytomas originate from neural stem/progenitor cells in a somatic tumor suppressor mouse model. Cancer cell. 15(1):45-56.
- Lu X, Feng X, Man X, Yang G, Tang L, Du D, Zhang F, Yuan H, Huang Q, Zhang Z, Liu Y. 2009. Aberrant splicing of Hugl-1 is associated with hepatocellular carcinoma progression. Clinical cancer research. 15(10):3287-96.
- Matsuda KI, Sato A, Okada M, Shibuya K, Seino S, Suzuki K, Watanabe E, Narita Y, Shibui S, Kayama T, Kitanaka C. 2012. Targeting JNK for therapeutic depletion of stem-like glioblastoma cells. Scientific reports. 2:516.
- McCubrey JA, Steelman LS, Abrams SL, Lee JT, Chang F, Bertrand FE, Navolanic PM, Terrian DM, Franklin RA, D'Assoro AB, Salisbury JL. 2006. Roles of the RAF/MEK/ERK and PI3K/PTEN/AKT pathways in malignant transformation and drug resistance. Advances in enzyme regulation. 46(1):249-79.
- Mechler BM, McGinnis W, Gehring WJ. 1985. Molecular cloning of lethal (2) giant larvae, a recessive oncogene of Drosophila melanogaster. The EMBO Journal. 4(6):1551-7.
- Menéndez J, Pérez-Garijo A, Calleja M, Morata G. 2010. A tumor-suppressing mechanism in Drosophila involving cell competition and the Hippo pathway. Proceedings of the National Academy of Sciences. 107(33):14651-6.
- Nakaya Y, Sheng G. 2013. EMT in developmental morphogenesis. Cancer letters. 341(1):9-15.

- Neumüller RA, Knoblich JA. 2009. Dividing cellular asymmetry: asymmetric cell division and its implications for stem cells and cancer. Genes & Development. 23(23):2675-99.
- Oh JE, Bae GU, Yang YJ, Yi MJ, Lee HJ, Kim BG, Krauss RS, Kang JS. 2009. Cdo promotes neuronal differentiation via activation of the p38 mitogen-activated protein kinase pathway. The FASEB Journal. 23(7):2088-99.
- Ohshiro T, Yagami T, Zhang C, Matsuzaki F. 2000. Role of cortical tumour-suppressor proteins in asymmetric division of Drosophila neuroblast. Nature. 408(6812):593.
- Orian JM, Vasilopoulos K, Yoshida S, Kaye AH, Chow CW, Gonzales MF. 1992. Overexpression of multiple oncogenes related to histological grade of astrocytic glioma. British journal of cancer. 66(1):106.
- Pal R, Mamidi MK, Das AK, Bhonde R. 2012. Diverse effects of dimethyl sulfoxide (DMSO) on the differentiation potential of human embryonic stem cells. Archives of toxicology. 86(4):651-61.
- Parsons LM, Portela M, Grzeschik NA, Richardson HE. 2014. Lgl regulates Notch signaling via endocytosis, independently of the apical aPKC-Par6-Baz polarity complex. Current Biology. 24(18):2073-84.
- Peng CY, Manning L, Albertson R, Doe CQ. 2000. The tumour-suppressor genes Lgl and Dlg regulate basal protein targeting in Drosophila neuroblasts. Nature. 408(6812):596.
- Phuphanick, S. 2017. Glioblastoma (GBM). *American Brain Tumor Association.*
- Rhee YH, Yi SH, Kim JY, Chang MY, Jo AY, Kim J, Park CH, Cho JY, Choi YJ, Sun W, Lee SH. 2016. Neural stem cells secrete factors facilitating brain regeneration upon constitutive Raf-Erk activation. Scientific reports. 6:32025.
- Ruan R, Zou L, Sun S, Liu J, Wen L, Gao D, Ding W. 2015. Cell blebbing upon addition of cryoprotectants: a self-protection mechanism. PloS one. 10(4):e0125746.
- Sabio G, Arthur JS, Kuma Y, Peggie M, Carr J, Murray-Tait V, Centeno F, Goedert M, Morrice NA, Cuenda A. 2005. p38γ regulates the localisation of SAP97 in the cytoskeleton by modulating its interaction with GKAP. The EMBO journal. 24(6):1134-45.
- Schaeffer HJ, Weber MJ. 1999. Mitogen-activated protein kinases: specific messages from ubiquitous messengers. Molecular and cellular biology. 19(4):2435-44.
- Shin K, Fogg VC, Margolis B. 2006. Tight junctions and cell polarity. Annual Review Cell Development Biology. 22:207-35.
- Singh SK, Hawkins C, Clarke ID, Squire JA, Bayani J, Hide T, Henkelman RM, Cusimano MD, Dirks PB. 2004. Identification of human brain tumour initiating cells. Nature. 432(7015):396.

- Song J, Peng XL, Ji MY, Ai MH, Zhang JX, Dong WG. 2013. Hugl-1 induces apoptosis in esophageal carcinoma cells both in vitro and in vivo. World journal of gastroenterology: World Journal of Gastroenterology. 19(26):4127.
- Sugiarto S, Persson AI, Munoz EG, Waldhuber M, Lamagna C, Andor N, Hanecker P, Ayers-Ringler J, Phillips J, Siu J, Lim DA. 2011. Asymmetry-defective oligodendrocyte progenitors are glioma precursors. Cancer cell. 20(3):328-40.
- Sun G, Irvine KD. 2013. Ajuba family proteins link JNK to Hippo signaling. Science Signalling. 6(292):ra81.
- Tanentzapf G, Tepass U. 2003. Interactions between the crumbs, lethal giant larvae and bazooka pathways in epithelial polarization. Nature cell biology. 5(1):46.
- Yoon CH, Kim MJ, Kim RK, Lim EJ, Choi KS, An S, Hwang SG, Kang SG, Suh Y, Park MJ, Lee SJ. 2012. c-Jun N-terminal kinase has a pivotal role in the maintenance of self-renewal and tumorigenicity in glioma stem-like cells. Oncogene. 31(44):4655.
- Yoshino Y, Aoyagi M, Tamaki M, Duan L, Morimoto T, Ohno K. 2006. Activation of p38 MAPK and/or JNK contributes to increased levels of VEGF secretion in human malignant glioma cells. International journal of oncology. 29(4):981-7.
- Zhu J, Blenis J, Yuan J. 2008. Activation of PI3K/Akt and MAPK pathways regulates Myc-mediated transcription by phosphorylating and promoting the degradation of Mad1. Proceedings of the National Academy of Sciences. 105(18):6584-9.

APPENDICES

Appendix A. Antibodies used for western blots. List of antibodies and their manufacturers and dilutions used for western blots.

Antibody	Dilution	Manufacturer	Catalog #
cJun	1:500	Abcam	31419/32137
p-cJun S63	1:500	Abcam	32385
cMyc	1:500	Cell Signaling	5605
p-p38	1:500	Cell signaling	9211
p38	1:500	Cell signaling	9212
p-ERK	1:500	Cell signaling	4370
ERK	1:500	Cell signaling	4695
p-JNK	1:1000	Abcam	124956
JNK	1:1000	Abcam	179461
Lgl	1:1000	Abcam	39292
CD133	1:500	Thermo Fisher	Pa5-38014
GAPDH	1:2000	Abcam	181602
2° Anti-Rb HRP	1:2000	Thermo Fisher	31460

Appendix B. Cell culture reagents and supplies. List of cell culture reagents and supplies used with catalog numbers and concentrations.

Reagent	Manufacturer	Catalog #	Concentration
Neurobasal-A	Gibco	10888022	1X
Vitamin B27 w/o Vit A	Gibco	12587010	1:50
L-glutamine	Gibco	25030081	1:100
EGF	Sigma-Aldrich	E9644	20 ug/mL
FGF	Pepro-tech	100-18B	20 ug/mL
Accutase	Corning	MT25058CI	--
Laminin	Corning	354239	6.1 ug/mL
Poly-O	Millipore	A-004-C	15 ug/mL
BIT 9500	STEMCELL	09500	1X
DMSO	Tocris	31-762	1:2000
SB203580	Adipogen	Syn-1074	10 uM
PD0325901	SelleckChem	S1036	1.0 uM
37 micron cell strainer	STEMCELL	27250	--

Appendix C. Reagents and kits used for immunoblots and proliferation assay. List of reagents and kits along with catalog numbers to perform immunoblots and proliferation assay.

Reagent/Kit	Manufacturer	Catalog #
NE-PER Nuclear and Cytoplasmic Extraction Reagents	Thermo Fisher	78835
Pierce BCA Protein Assay Kit	Thermo Fisher	23227
Bovine serum albumin	Thermo Fisher	BP9706100
CyQuant NF Cell Proliferation Assay Kit	Invitrogen	C35006
Novex Tris-Glycine 10-20% gels	Invitrogen	XP1020_
PVDF membrane	Millipore	IPVH00010
WesternSure Premium Chemiluminescent Substrate	Li-Cor	C50528-02
Stripping Buffer	Thermo Fisher	21059

Appendix D. Viability of neurospheres harvested for adherent assays was consistently above 92%. Percent viability of neurospheres harvested for adherent culture assays.

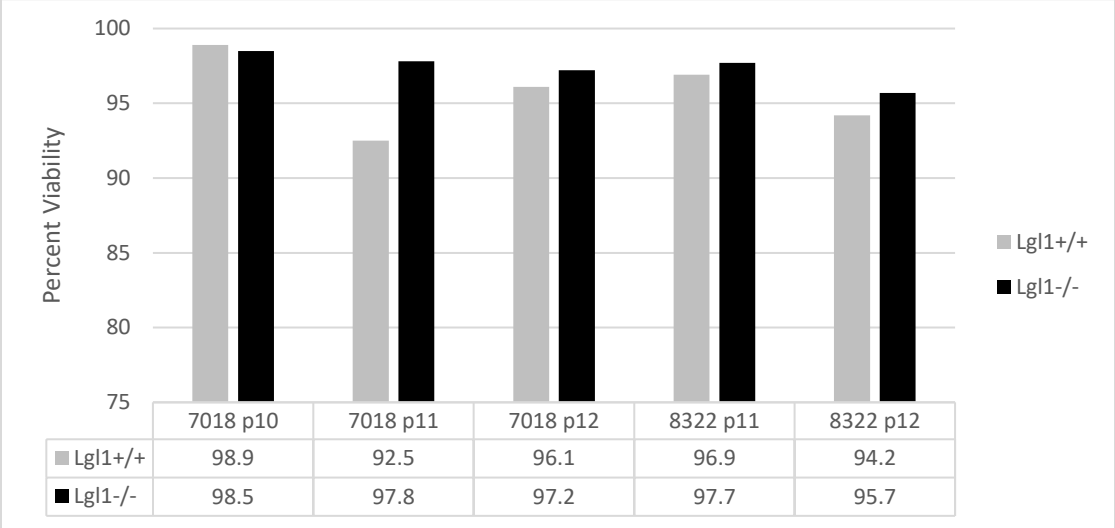

	7018 p10	7018 p11	7018 p12	8322 p11	8322 p12
Lgl1+/+	98.9	92.5	96.1	96.9	94.2
Lgl1-/-	98.5	97.8	97.2	97.7	95.7

Appendix E. Counts and proliferation of neurospheres prior to harvesting for adherent culture assays. Proliferation of spheres prior to harvesting for adherent culture. All replicates were propagated for 5 days except 8322 p12 for 6 days due to slow and abnormal growth. Cells seeded and harvest are in millions of cells. Growth is referred to as harvested over seeded values. Fold change defined as $Lgl1^{-/-}/Lgl1^{+/+}$ of growth values.

Sphere Proliferation										
	7018						8322			
	P10		P11		P12		P11		P12	
	$Lgl1^{-/-}$	$Lgl1^{+/+}$	$Lgl1^{-/-}$	$Lgl1^{+/+}$	$Lgl1^{-/-}$	$Lgl1^{+/+}$	$Lgl1^{-/-}$	$Lgl1^{+/+}$	$Lgl1^{-/-}$	$Lgl1^{+/+}$
Cells seeded	0.80	1.01	1.22	0.94	1.00	1.00	1.08	1.32	1.00	1.00
Cells harvested	12.42	20.45	11.70	14.81	18.06	18.87	11.99	20.00	14.22	13.39
Growth	15.48	20.35	9.56	15.79	18.06	18.87	11.12	15.13	14.22	13.39
Fold Change	1.31		1.65		1.05		1.36		0.94	

Appendix F. Western blots for all replicates of phosphorylated c-Jun and c-Jun. Western blots on nuclear extracts from adherent cultures normalized to GAPDH on c-Jun and phosphorylated c-Jun (Ser63). Labels are defined as follows: no treatment (NT), DMSO at 1:2000 (DMSO), 10 μM SB203580 (SB10), 1.0 μM PD0325901 (PD1.0).

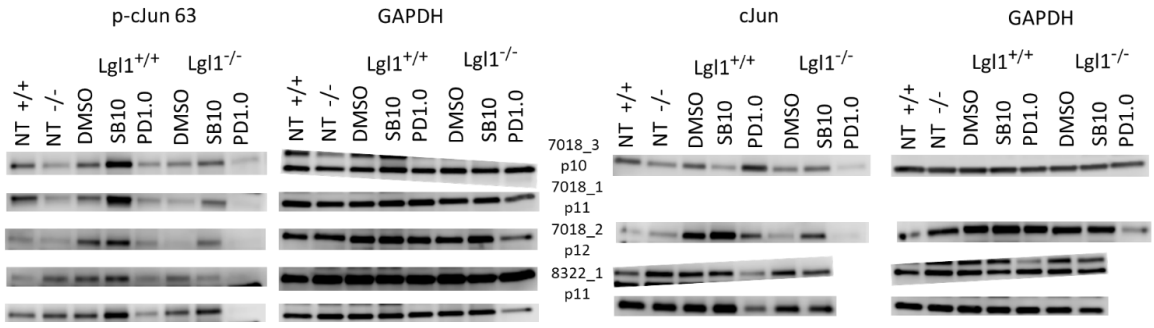

Appendix G. Western blots for all replicates of c-Myc. Western blots on nuclear extracts from adherent cultures normalized to GAPDH on c-Myc. Labels are defined as follows: no treatment (NT), DMSO at 1:2000 (DMSO), 10 μM SB203580 (SB10), 1.0 μM PD0325901 (PD1.0).

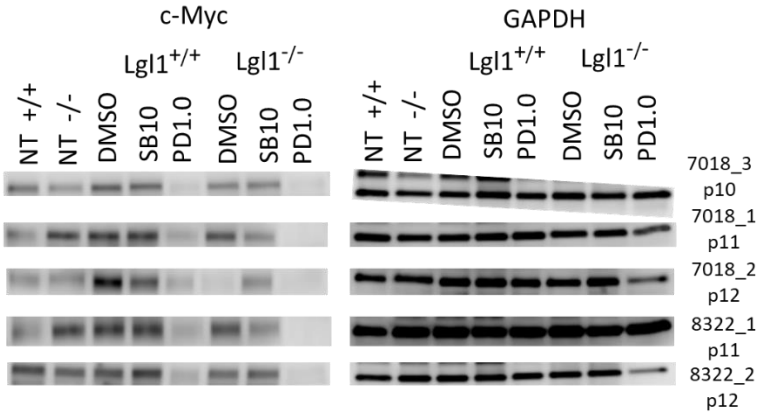

Appendix H. Western blots for all replicates of phosphorylated p38 and p38. Western blots on cytoplasmic extracts from adherent cultures normalized to GAPDH on p38 and phosphorylated p38 (Thr180/Tyr182). Labels are defined as follows: no treatment (NT), DMSO at 1:2000 (DMSO), 10 μM SB203580 (SB10), 1.0 μM PD0325901 (PD1.0).

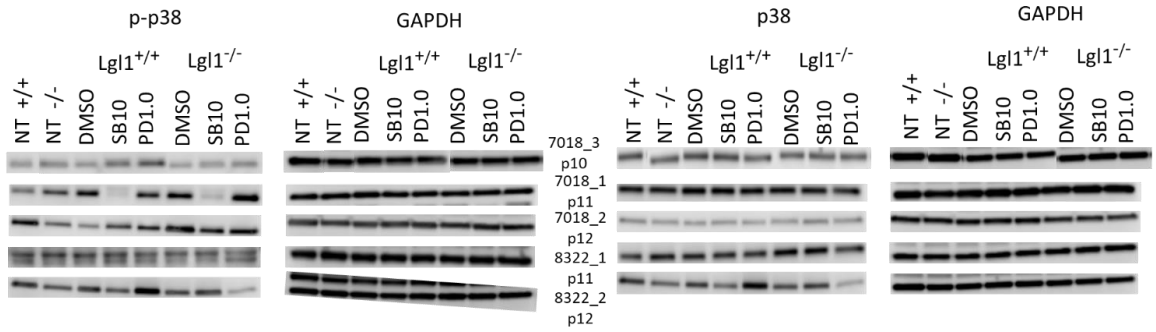

Appendix I. Western blots for all replicates of phosphorylated ERK and ERK. Western blots on cytoplasmic extracts from adherent cultures normalized to GAPDH on ERK1/2 p44/42 and phosphorylated ERK1/2 (Thr202/Tyr204). Labels are defined as follows: no treatment (NT), DMSO at 1:2000 (DMSO), 10 μM SB203580 (SB10), 1.0 μM PD0325901 (PD1.0).

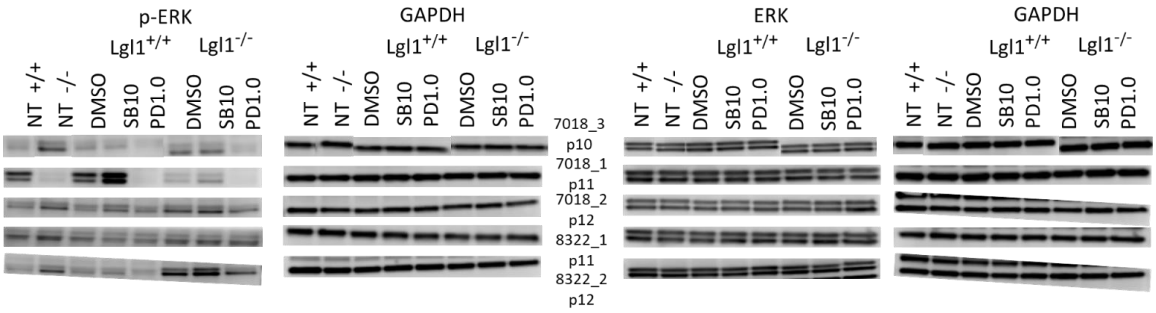

Appendix J. Western blots for all replicates of phosphorylated JNK and JNK. Western blots on cytoplasmic extracts from adherent cultures normalized to GAPDH on JNK1/2/3 p54/46 and phosphorylated JNK1/2/3 (Thr183/Thr183/Thr221). Labels are defined as follows: no treatment (NT), DMSO at 1:2000 (DMSO), 10 µM SB203580 (SB10), 1.0 µM PD0325901 (PD1.0).